STEM CELLS AND DEVELOPMENT
Volume 24, Number 13, 2015
© Mary Ann Liebert, Inc.
DOI: 10.1089/scd.2014.0588

VAV3 Overexpressed in Cancer Stem Cells Is a Poor Prognostic Indicator in Ovarian Cancer Patients

Ah-Young Kwon,[1] Gwang-Il Kim,[1,2] Ju-Yeon Jeong,[2] Ji-Ye Song,[2] Kyu-Beom Kwack,[3] Chan Lee,[4] Hae-Youn Kang,[1,2] Tae-Heon Kim,[1,2] Jin-Hyung Heo,[1,2] and Hee Jung An[1,2]

Ovarian carcinoma is a highly lethal malignancy due to frequent relapse and drug resistance. Cancer stem cells (CSCs) are thought to contribute significantly to disease relapse and drug resistance. In this study, a subpopulation of CSCs of ovarian carcinoma was isolated and the genes differentially expressed in these cells were identified to characterize CSCs and to find candidate biomarkers. Ovarian carcinoma cells from patients were primarily cultured, and spheroid-forming cells (SFCs) were isolated. The characteristic genes of SFCs were identified through cDNA microarray and validation by quantitative real-time polymerase chain reaction and immunohistochemistry, and the association of their expression with clinicopathologic parameters was analyzed. *GSC* (4.26-fold), *VAV3* (7.05-fold), *FOXA2* (12.06-fold), *LEF1* (17.26-fold), *COMP* (21.33-fold), *GRIN2A* (9.36-fold), *CD86* (23.14-fold), *PYY* (4.18-fold), *NKX3-2* (10.35-fold), and *PDK4* (74.26-fold) were significantly upregulated in SFCs compared with parental cancer cells. With validation for human ovarian carcinomas, *LEF1*, *PYY*, *NKX3-2*, and *WNT3A* were significantly upregulated in chemoresistant cancers compared with chemosensitive cancers. Overexpression of LEF1, VAV3, and NKX3-2 was significantly associated with distant metastasis by immunohistochemistry. VAV3 overexpression was an independent poor survival indicator (hazard ratio = 15.27, $P < 0.05$) by multivariate Cox analysis. The further functional assay revealed that *VAV3* knockdown regulated CSC activation and ovarian cancer cell proliferation and sensitized paclitaxel (PTX)-resistant cancer cells to PTX treatment. Taken together, we identified by high-throughput analysis of CSCs that VAV3 overexpression is a novel biomarker for poor prognosis and survival in ovarian carcinoma.

Introduction

Ovarian carcinoma is the highest lethal cancer among female malignancies. The high mortality of ovarian carcinoma results from chemoresistance and frequent recurrence after initial treatment. Despite the development of novel molecular targeting agents to prevent disease progression, ovarian carcinoma still has a high rate of recurrence and mortality; thus, an improved understanding of the mechanisms for chemoresistance and recurrence is crucial.

Recently, interest in cancer stem cells (CSCs) has been increasing because CSCs, a small population of cells within tumors that have tumorigenic capacity [1], are thought to have an impact on recurrence and chemoresistance [2,3]. CSCs have three main properties: (i) they express distinct surface markers; (ii) they are selectively endowed with tumorigenic capacity; and (iii) they sustain the growth of heterogeneous cancer tissues, therefore, displaying two of the functional hallmarks of stem cells, namely self-renewal and differentiation into multiple cell types [4–7]. CSCs also contribute to cancer recurrence through their resistance to anticancer drugs and their tumorigenic capacity, and many previous studies show that CSCs can resist chemoradiation therapy [6–9]. Moreover, initial chemotherapy increases the proportion of drug-resistant CSCs, resulting in cancer recurrence [10]. Therefore, it is important to understand the characteristics of ovarian CSCs to predict and treat cancer recurrences. Indeed, ovarian CSCs have been studied in a variety of ways; however, no effective strategies to reduce ovarian CSCs have been developed yet.

In the present study, we therefore sought to identify the characteristic genes in ovarian CSCs and to investigate the clinical significance of these genes in high-grade ovarian serous carcinoma (OSC), which is the most common and aggressive type of ovarian carcinoma and is responsible for 90% of ovarian cancer deaths [11]. CSCs were first isolated from fresh OSC tumors by spheroid formation assay, and the genes differentially expressed in the CSCs were investigated by high-throughput cDNA microarray and quantitative real-time polymerase chain reaction (qRT-PCR). The mRNA and protein expression levels of these genes were confirmed in OSC samples and correlated with clinicopathologic parameters to assess the clinical impact of these genes and to identify candidate biomarkers for patient outcome.

[1]Department of Pathology, [2]Institute for Clinical Research, [3]Department of Biomedical Science, and [4]Department of Gynecologic Oncology, College of Medicine, CHA University, Sungnam, Republic of Korea.

Materials and Methods

Patients and tissue samples

For isolation and evaluation of CSCs, the tumor cells of high-grade OSCs were primarily cultured at the time of surgery from 17 patients who had undergone oophorectomy for ovarian carcinoma. A spheroid formation assay was performed using cultured primary cancer cells.

For qRT-PCR to validate mRNA expression for differentially expressed genes in the cDNA microarray, 36 fresh tissues of high-grade OSCs, which were obtained at the time of surgery from patients undergoing oophorectomy, were used. Table 1 shows the clinicopathological characteristics of these patients. Fallopian tubes from patients undergoing hysterectomy with salpingectomy due to benign leiomyoma were used as healthy controls.

For immunohistochemical (IHC) analysis, formalin-fixed paraffin-embedded tissues from 74 high-grade OSC patients treated at the Bundang CHA Medical Center were used. The clinicopathologic characteristics of these patients are shown in Table 1. The histologic diagnosis and clinical stage were according to the World Health Organization (WHO) classification. Histopathologic grading was assessed according to a two-tiered grading system, and tumor staging was carried out according to the tumor–node–metastasis staging system. The samples were divided into chemosensitive and chemoresistant groups according to responsiveness to first-line chemotherapy (taxol/platinum-based combination therapy) after surgery.

Our study was approved by the Ethics Committee of the Bundang CHA Medical Center, and informed consent was obtained from all patients.

Table 1. The Clinicopathological Characteristics of the Cases Used for Quantitative Real-Time Polymerase Chain Reaction Analysis and Immunohistochemical Staining

	Total	*Chemosensitive*	*Chemoresistant*
qRT-PCR analysis			
Age (years)	57.4 ± 11.3	56.6 ± 11.3	58.8 ± 11.7
Stage			
I/II (%)	5 (13.9)	5 (21.7)	0 (0)
III/IV (%)	31 (86.1)	18 (78.3)	13 (100)
Nodal metastasis			
Absent (%)	17 (47.2)	11 (47.8)	6 (46.2)
Present (%)	19 (52.8)	12 (52.2)	7 (53.8)
Distant metastasis			
Absent (%)	26 (72.2)	16 (69.6)	10 (76.9)
Present (%)	10 (27.8)	7 (30.4)	3 (23.1)
Total (%)	36	23 (68.9)	13 (36.1)
IHC analysis			
Age (years)	53.8 ± 10.4	52.0 ± 9.8	59.2 ± 10.4
Stage			
I/II (%)	14 (18.9)	14 (25.5)	0 (0)
III/IV (%)	60 (81.1)	41 (74.5)	19 (100)
Nodal metastasis			
Absent (%)	35 (47.3)	28 (50.9)	7 (36.8)
Present (%)	39 (52.7)	27 (49.1)	12 (63.2)
Distant metastasis			
Absent (%)	38 (51.4)	30 (54.5)	8 (42.1)
Present (%)	36 (48.6)	25 (45.5)	11 (57.9)
Recurrence			
Absent (%)	34 (45.9)	29 (52.7)	5 (26.3)
Present (%)	40 (54.1)	26 (47.3)	14 (73.7)
Total (%)	74	55 (74.3)	19 (25.7)

IHC, immunohistochemistry; qRT-PCR, quantitative real-time polymerase chain reaction.

Primary cell culture and spheroid-forming cell isolation

Primary tumor cells were obtained at the time of surgery from 17 high-grade OSC patients who had undergone oophorectomies. Tumors were mechanically dissected into small pieces and enzymatically digested into single-cell suspensions and incubated at 37°C for 1 h in Ca^{2+}/Mg^{2+}-free phosphate-buffered saline containing 50 U/mL collagenase A (Roche, Pleasanton, CA). Cells were incubated with Ber-EP4-coated magnetic Dynabeads (Life Technologies, Grand Island, NY) for 30 min to select epithelial cells, which were then cultured in RPMI medium (Gibco/Life Technologies, Grand Island, NY) containing 10% fetal bovine serum, 1% penicillin–streptomycin, and 20 ng/mL epidermal growth factor (Life Technologies). For the spheroid formation assay, single cells were plated on ultralow-attachment six-well culture plates (Corning, Acton, MA) at a density of 1×10^3 cells/cm^2 in serum-free Dulbecco's modified Eagle's medium/F12 medium (Life Technologies) supplemented with 20 ng/mL epidermal growth factor (Life Technologies), 10 ng/mL basic fibroblast growth factor (Sigma-Aldrich, St Louis, MO), 0.4% bovine serum albumin (Sigma-Aldrich), and 5 μg/mL insulin (Sigma-Aldrich). Spheroid formation of 50–100 cells was assessed at 7 days after seeding. The spheroid-forming efficiency was defined as the ratio of colonies/cells seeded per well.

cDNA microarray analysis

The cDNA microarray was performed on four spheroid-forming cell (SFC) samples and the corresponding primary cancer cells. The cDNA was obtained using the iScript cDNA synthesis kit (Bio-Rad, Reymond, WA). The synthesis of target cRNA probes and the hybridization were performed using Agilent's Low RNA Input Linear Amplification kit (Agilent Technology, Santa Clara, CA). Amplified and labeled cRNA was purified on the cRNA Cleanup Module (Agilent Technology). The fragmented cRNA was directly pipetted onto assembled Human Oligo Microarrays (60K) (Aligent Technology).

The hybridized images were scanned using a DNA microarray scanner and quantified with Feature Extraction Software (Agilent Technology). Data normalization and selection of significantly changed genes were performed using GeneSpring GX 7.3 (Agilent Technology). The averages of normalized ratios were calculated by dividing the average normalized signal channel intensity by the average normalized control channel intensity. Functional annotation of genes was performed according to the Gene Ontology Consortium (www.geneontology.org/index.shtml) by GeneSpring GX 7.3. Gene classification was based on DAVID (http://david

.abcc.ncifcrf.gov/) and on Medline databases (www.ncbi.nlm.nih.gov/).

Quantitative real-time polymerase chain reaction

Total RNA was isolated from tissue or primary cells using TRIzol reagent (Life Technologies). First-strand cDNA synthesis was performed using the Superscript III kit (Life Technologies). Real-time PCR was conducted in triplicate using the CFX96 Real-Time PCR Detection System (Bio-Rad Laboratories, Hercules, CA). The final reaction volume of 20 μL included 0.5 μL of cDNA template, 10 μL of TaqMan Master Mix (Applied Biosystems, Paisley, United Kingdom), and 1 μL of a mix containing primers and probes. Transcript levels were normalized versus glyceraldehyde 3-phosphate dehydrogenase (*GAPDH*) expression. The gene expression was calculated using the formula $2^{-\Delta\Delta Ct}$.

Tissue microarray and IHC staining

For IHC analysis, 74 OSC cases were used to construct a tissue microarray. For each case, two tissue cores with diameters of 3 mm were punched out from each donor tissue block and arranged into recipient paraffin blocks using a manual microarray device (UNITMA; Quick-RAY™ UNI-Tech Science, Seoul, Korea). Tissue microarray paraffin sections were deparaffinized in xylene. Endogenous peroxidase activity was blocked with 0.3% hydrogen peroxide. For antigen retrieval, the sections were heated in 0.1 M citrate buffer (pH 6.0) for 15 min in a microwave oven. Slides were incubated overnight at 4°C with the following primary antibodies and working dilutions: FOXA2 (1:200; Abcam, Cambridge, United Kingdom), LEF1 (1:250; Abcam), PYY (1:50; Abcam), VAV3 (1:50; Novus Biologicals, Littleton, CO), NKX3-2 (1:75; Novus Biologicals), and Wnt3A (1:750; Novus Biologicals). Slides were then incubated with the secondary antibody for 15–30 min using the HRP Polymer Ultravision LP Detection System (Thermo Scientific, Waltham, MA) at room temperature. The sections were then developed with diaminobenzidine and counterstained with hematoxylin. The IHC stains were interpreted by two independent pathologists.

Protein expression was determined by an immunoreactive score. The percentage of positive cells was scored as 0 (negative), 1 (<10% positive cells), 2 (10%–50% positive cells), 3 (51%–75% positive cells), or 4 (>75% positive cells). The staining intensity was categorized as 0 (negative), 1 (weak), 2 (moderate), or 3 (strong). The final immunoreactive score was calculated by multiplying these two scores.

Functional assay for VAV3

Transfection of VAV3 siRNA. For functional assay, we used paclitaxel (PTX)-resistant SKpac cells, which were generated by continuous exposure of SKOV3 (ATCC, Manassas, VA) cells to a stepwise escalating concentration of PTX over 8 months [12]. *VAV3* siRNA and negative siRNA for control (Supplementary Table S1; Supplementary Data are available online at www.liebertpub.com/scd) were synthesized by Invitrogen (Carlsbad, CA). The day before transfection, 1×10^5 cells were seeded into each well of a six-well plate. The next day, cells were transfected with annealed siRNA oligos using Lipofectamine 2000 (Invitrogen) according to the manufacturer's instructions. At 24 and 48 h after transfection, cells were harvested, and the efficiency of *VAV3* knockdown after siRNA transfection was confirmed by qRT-PCR. The cells were prepared for subsequent studies, including MTT, colony forming, and spheroid-forming assays.

MTT assay for cell viability

Cells (1×10^4) were seeded in a 96-well culture plate and subsequently treated with 10 pmol *VAV3* siRNA in culture medium for 24 and 48 h. Control cells were treated with 10 pmol negative siRNA in culture medium. After 24 and 48 h, the cells were incubated with MTT reagent (0.5 mg/mL) at 37°C for 4 h. The resulting formazan crystals were solubilized by the addition of 100 μL DMSO to each well.

Colony-forming assay

Cells were seeded at a density of 1×10^5 cells per well in six-well plates. The next day, cells were transfected with siRNA and incubated for 48 h. Transfected cells were then replated at 300 cells per well in a gelatin-coated six-well culture dish. After 14 days, colonies were visualized using hematoxylin after fixation with 4% paraformaldehyde for 10 min and then counted. Groups of >50 cells were scored as colonies.

Statistical analysis

Statistical analysis was conducted using the SPSS statistics software package (IBM SPSS Statistics Data Editor 20). The associations between mRNA and protein expression levels in each tumor group and clinicopathologic factors were evaluated by χ^2 analysis, Fisher's exact test, or the Mann–Whitney test. For survival analysis, the Kaplan–Meier method and the Cox proportional hazards model were used. The results of each functional assay are expressed as mean ± standard error. Student's *t*-test was performed and $P < 0.05$ was considered significant.

Results

Cancer stem cells were enriched in SFCs isolated from the primary cell culture of human ovarian carcinoma tissue

The nonadherent spherical clusters of 50–100 cells were observed 1 week after plating on spheroid-forming assay (Fig. 1A). The SFCs were collected, and the spheroid-forming capacity was assessed. The efficiency of spheroid formation from the inoculated cells was 2.37% ± 0.4% in the first generation. These floating spheres were enzymatically dissociated, and single cells were harvested and used to form secondary spheroids under the same culture conditions. The spheroid-forming capacity in the second generation was similar to the first (2.17% ± 0.3%) (Fig. 1B and Table 2).

To examine whether the CSCs were enriched in SFCs, the mRNA expression of the well-known stem cell marker was analyzed in the SFCs by qRT-PCR and compared with that of the parental primary cancer cells. The stem cell markers that were evaluated in this study are *ALDH1* [13], *CD24* [13], *CD44* [14], CD133 [15], *NOTCH3* [4], *SOX2* [13], and *CD117* [14]. All of these stem cell markers, except *CD117*, were more highly expressed in the SFCs than in the primary cancer cells (Fig. 1C, $P < 0.05$), suggesting that CSCs were

enriched in the cells capable of forming spheroids. Therefore, we refer to these cells as CSC-like cells.

Gene expression profiles of CSC-like cells by cDNA microarray

A cDNA microarray was performed to evaluate the gene expression profile of the spheroid-forming CSC-like cells. Gene expression was compared between four CSC-like cell samples and their corresponding parental primary cancer cells. The expression of 619 genes was significantly increased or decreased at least 5-fold in the CSC-like cells ($P < 0.05$). Among these genes, 381 were increased and 238 genes were decreased compared with parental cancer cells. Hierarchical clustering of 62 genes that were significantly altered more than 15-fold in CSC-like cells is shown in Fig. 2A. The microarray data presented here were prepared according to minimum information about a microarray

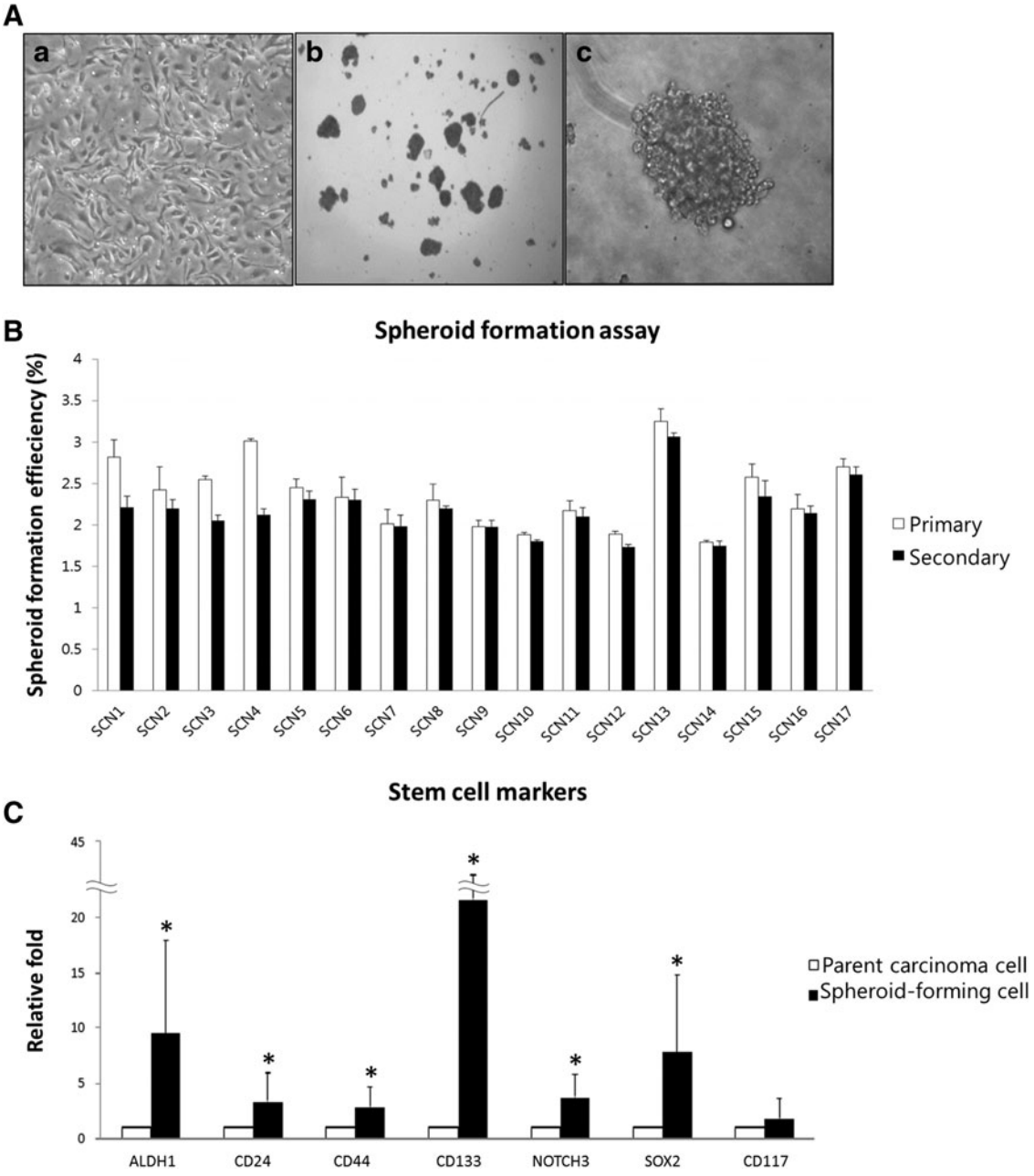

FIG. 1. Isolation of cancer stem cells (CSCs) from cultured primary cells from 17 ovarian serous carcinomas (OSCs) by spheroid formation assay. **(A)** Phase-contrast image of primary culture of OSC cells **(a)** and spheroid morphology with low **(b)** and high **(c)** power view. **(B)** The spheroid-forming capacity of the primary cancer cells was consistent (2.17%–2.37%) between the first and second generations, indicating that the spheroid-forming cells (SFCs) had self-renewing characteristics. **(C)** Significant expression of stem cell markers was detected in SFCs (*$P < 0.05$). Known markers of stem cells were used, and all markers, except *CD117*, were significantly overexpressed in SFCs, indicating that the SFCs are enriched in CSCs compared with the cultured primary cells.

Table 2. The Primary and Secondary Spheroid-Forming Capability of Ovarian Serous Carcinoma Cells

	Primary (%)	*Secondary (%)*
SCN1	2.82	2.21
SCN2	2.42	2.2
SCN3	2.55	2.05
SCN4	3.01	2.12
SCN5	2.45	2.31
SCN6	2.33	2.3
SCN7	2.01	1.98
SCN8	2.3	2.19
SCN9	1.98	1.97
SCN10	1.88	1.8
SCN11	2.17	2.1
SCN12	1.89	1.73
SCN13	3.25	3.06
SCN14	1.79	1.75
SCN15	2.57	2.34
SCN16	2.19	2.14
SCN17	2.7	2.61
Mean ± SD	2.37 ± 0.4	2.17 ± 0.3

SCN, serous carcinoma; SD, standard deviation.

experiment (MIAME) recommendations and are accessible through Gene Expression Omnibus (GEO) Series accession number GSE60765 (www.ncbi.nlm.nih.gov/geo).

The genes that were increased or decreased at least 2-fold in CSC-like cells ($P < 0.05$) were classified according to biological process gene ontology. A pie chart showing the proportion of genes representing each process is shown in Fig. 2B. The greatest number of genes were associated with apoptosis and proliferation (13% each), followed by cell cycle (10%); CSCs (8%) and signal transduction (8%); transforming growth factor-β (6%), mitogen-activated protein kinase (6%), tyrosine kinase (6%), and Notch signaling (6%); drug response (5%) and Wnt signal transduction (5%); hedgehog signaling (4%); epithelial–mesenchymal transition (3%) and Toll-like signaling (3%); and the insulin receptor pathway (2%). Among the CSC markers, *CD24* (13.85-fold), *ALDH1A1* (6.80-fold), and *SOX2* (5.36-fold) were significantly upregulated in spheroid-forming CSC-like cells. The oncogenesis-associated genes that were increased more than 5-fold in CSC-like cells compared with parental cancer cells are summarized in Table 3 along with their associated functions.

Selection of 14 genes as candidate biomarkers and validation by qRT-PCR

To identify candidate biomarkers for predicting poor prognosis and chemoresistance, 14 genes were selected for qRT-PCR validation based on the results of the cDNA microarray and gene ontology. From the genes upregulated more than 5-fold in CSC-like cells by cDNA microarray, the most highly expressed genes from each gene ontology category that are associated with oncogenesis were selected for further study. The relative expression levels of these 14 genes by cDNA microarray were as follows: *GSC* (8.39-fold), *VAV3* (11.75-fold), *FOXA2* (15.11-fold), *LEF1* (28.76-fold), *COMP* (15.34-fold), *AZU1* (13.36-fold), *GRIN2A* (7.34-fold), *IL17F* (17.36-fold), *CD86* (8.67-fold), *PYY* (11.98-fold), *FIGF* (14.01-fold), *NKX3-2* (9.43-fold), *WNT3A* (6.19-fold), and *PDK4* (11.83-fold).

The mRNA expression of these 14 genes was validated by qRT-PCR for 17 sets of SFCs and their parental cancer cells. *GSC* (4.26-fold; $P < 0.001$), *VAV3* (7.05-fold; $P < 0.001$), *FOXA2* (12.06-fold; $P < 0.05$), *LEF1* (17.26-fold; $P < 0.05$), *COMP* (21.33-fold; $P < 0.001$), *GRIN2A* (9.36-fold; $P < 0.001$), *CD86* (23.14-fold; $P < 0.001$), *PYY* (4.18-fold; $P < 0.001$), *NKX3-2* (10.35-fold; $P < 0.001$), and *PDK4* (74.26-fold; $P < 0.001$) were significantly upregulated in SFCs compared with parental cancer cells (Fig. 2C). The expression of *AZU1* (1.60-fold), *IL17F* (5.24-fold), *FIGF* (11.22-fold), and *WNT3A* (11.17-fold) was also highly increased in SFCs compared with their corresponding parental cancer cells; however, these differences were not statistically significant.

LEF1, PYY, NKX3-2, and WNT3A were upregulated in chemoresistant cancers compared with chemosensitive cancers

We performed qRT-PCR to assess the mRNA expression of these candidate genes in 36 fresh human OSC tissues. *GSC* was excluded from this study because we previously reported that *GSC* mRNA was significantly upregulated in chemoresistant OSCs compared with chemosensitive carcinomas, and GSC protein expression was associated with poor prognosis in OSC [16]. The mRNA expression levels were compared in OSC tissue and control tissue obtained from normal fallopian tubes, which are known to be the origin of OSC [17–19].

In the human OSC, 11 genes were significantly highly overexpressed by qRT-PCR compared with controls as follows: *VAV3* (7.92-fold), *FOXA2* (7.32-fold), *LEF1* (9.64-fold), *COMP* (25.01-fold), *GRIN2A* (12.51-fold), *IL17F* (2.50-fold), *CD86* (6.35-fold), *PYY* (13.50-fold), *NKX3-2* (10.79-fold), *WNT3A* (15.67-fold), and *PDK4* (10.19-fold) (all $P < 0.05$). Figure 3A shows the relative expression of 13 candidate genes in OSCs and controls. When expression levels in chemoresistant and chemosensitive cancers were compared, significant differences were found for *LEF1*, *PYY*, *NKX3-2*, and *WNT3A* ($P < 0.05$). *LEF1* was upregulated 2.85-fold in chemoresistant cancers compared with chemosensitive cancers; *PYY* was upregulated 20.03-fold; *NKX3-2*, 3.02-fold; and *WNT3A*, 3.91-fold (Fig. 3B). Additionally, the correlation between mRNA expression levels and clinicopathologic parameters was analyzed. The upregulation of *VAV3* (>2-fold relative to normal controls) correlated with distant metastasis ($P < 0.05$). *PYY* upregulation (>2-fold) correlated with lymph node metastasis ($P < 0.05$) and chemoresistance ($P < 0.05$). The upregulation of *FoxA2* (>6-fold) and *NKX3-2* (>10-fold) was associated with chemoresistance ($P < 0.05$, respectively) (Fig. 3C).

The overexpression of VAV3, NKX3-2, and LEF1 was associated with poor prognostic parameters in OSCs

An IHC study was performed on a tissue microarray of 74 OSC cases to validate the protein expression of candidate genes and to assess the association between the protein

expression of these genes and clinicopathologic parameters, such as clinical stage, nodal and distant metastases, chemoresistance, and survival. Six proteins were selected for IHC analysis, namely LEF1, PYY, NKX3-2, and WNT3A, which were significantly upregulated at the mRNA level in chemoresistant compared with chemosensitive OSCs, and VAV3 and FOXA2, for which the mRNA levels showed clinicopathological significance.

Staining was observed in the cytoplasm or the nucleus of OSC tissue, focally or diffusely (Fig. 4A). FOXA2, LEF1, and NKX3-2 showed nuclear positivity, PYY showed cytoplasmic positivity, and VAV3 showed both nuclear and cytoplasmic positivity. The epithelial and stromal cells of benign serous cystadenomas and normal fallopian tubes were negative or weakly positive (less than 5% positive cells) for FOXA2, LEF1, NKX3-2, and VAV3. Apical staining for Wnt3A was found in epithelial cells of normal fallopian tubes and benign serous cystadenomas, while in OSC tissue, membranous staining was observed, and it was considered positive if staining was completely membranous. LEF1, NKX3-2, PYY, and Wnt3A were considered overexpressed when the immunoreactive score was ≥ 4; FOXA2 was considered overexpressed when the immunoreactive score was ≥ 2; and VAV3 was considered overexpressed when the immunoreactive score was ≥ 6.

The majority of OSCs overexpressed these proteins. FOXA2 was overexpressed in 66.2% (49/74) of cases, and LEF1 was overexpressed in 59.5% (44/74) of cases. VAV3 was overexpressed in 75.7% (56/74) of OSCs, and overexpression of PYY, NKX3-2, and Wnt3A was observed in 58.1% (43/74), 58.1% (43/74), and 63.5% (47/74) of cases, respectively. The associations between IHC staining and clinicopathologic parameters are shown in Table 4. Distant metastasis was significantly associated with the expression of LEF1, VAV3, and NKX3-2 ($P < 0.05$, respectively). Chemoresistance significantly correlated with overexpression of NKX3-2 ($P < 0.05$).

High VAV3 immunoreactivity was an independent poor prognostic indicator in OSCs

A survival analysis was performed for 74 OSC patients according to their protein expression by immunohistochemistry. The median follow-up period was 31 months (range, 1–112 months). During the follow-up period, 21 patients (28.4%) died of disease. The Kaplan–Meier analysis (Fig. 4B) revealed that overexpression of VAV3 (immunoreactive score ≥ 6) and FOXA2 (immunoreactive score ≥ 2) was significantly associated with shorter overall survival (OS) (VAV3, OS: 64.2% vs. 94.4%, $P < 0.05$; FOXA2, OS: 63.3% vs. 88%, $P < 0.05$). The expression of the other proteins was not associated with patient survival.

A multivariate Cox regression analysis was performed for clinicopathological parameters and VAV3 and FOXA2 immunoreactivity. VAV3 overexpression was an independent indicator of poor survival in OSC patients (Table 5; hazard ratio = 15.27, $P < 0.05$), suggesting that VAV3 overexpression could be a novel poor prognostic factor in OSC; however, FOXA2 overexpression was not significantly associated with OS in this analysis. As expected, chemoresistance was also associated with poor survival (hazard ratio = 17.74, $P < 0.001$).

VAV3 knockdown inhibits spheroid formation and decreases cancer cell viability and proliferation

With *VAV3* siRNA treatment, the mRNA levels of *VAV3* at 24 and 48 h were significantly downregulated to 35% and 38% of the control ($P < 0.005$), respectively (Supplementary Fig. S1). To verify the effect on CSC activation by *VAV3* siRNA, the spheroid-forming ability was assessed by spheroid-forming assay. We compared the *VAV3* knockdown cells with controls for the number and size of the spheroids. The number of spheroid formations decreased significantly after treatment of *VAV3* siRNA (30% decrease compared with negative siRNA control, $P < 0.001$). The size of the spheroids was also markedly reduced as shown in Fig. 5A, indicating that *VAV3* knockdown inhibits CSC activation.

The colony-forming assay showed that clonal growth of SKpac cells was significantly inhibited by *VAV3* siRNA. The number of colonies of SKpac cells treated with *VAV3* siRNA decreased by 41% ($P < 0.001$) compared with the cells treated with negative siRNA (Fig. 5B).

To assess the effect of *VAV3* inhibition on sensitivity to PTX of PTX-resistant SKpac cells, we examined cell viability using MTT assay. Inactivation of *VAV3* by siRNA treatment enhanced the sensitivity of SKpac cells to PTX treatment. Cell viability decreased by 25% and 18% ($P < 0.05$) at 24 and 48 h, respectively, in SKpac cells treated with *VAV3* siRNA compared with the negative siRNA control. With *VAV3* siRNA and 40 nM PTX treatment, the number of SKpac cells decreased by 27% ($P < 0.05$) and

FIG. 2. cDNA microarray analysis of OSC SFCs and the corresponding primary cancer cells. **(A)** Hierarchical clustering of significantly altered genes with a ≥ 15-fold difference between SFCs and primary cancer cells. The clustered expression data are displayed on a heat map, with individual samples and genes listed on the X-axis and Y-axis, respectively. The gray-scale depicted the relative levels of gene expression in SFC samples compared with their corresponding primary cancer cells from *light* (for higher up- or down-regulation) to *dark* (for lower up- or down-regulation). Twenty-eight genes were highly expressed in all four of the SFC samples compared with control cells. Thirty-four genes were downregulated in all four SFC samples compared with control cells. **(B)** Pie chart showing the ontology of the genes that were up- or downregulated more than 2-fold in SFCs ($P < 0.05$). Genes associated with apoptosis and proliferation each account for 13% of the differentially expressed genes, genes associated with the cell cycle account for 10%, genes associated with signal transduction and CSCs each account for 8%, and genes involved in the drug response account for 5% of the differentially expressed genes. **(C)** Validation by quantitative real-time polymerase chain reaction (qRT-PCR) of genes that were significantly upregulated by cDNA microarray. The qRT-PCR on 17 sets of SFCs and parental cancer cells found that *GSC* (4.26-fold), *VAV3* (7.05-fold), *FOXA2* (12.06-fold), *LEF1* (17.26-fold), *COMP* (21.33-fold), *GRIN2A* (9.36-fold), *CD86* (23.14-fold), *PYY* (4.18-fold), *NKX3-2* (10.35-fold), and *PDK4* (74.26-fold) were significantly upregulated in SFCs compared with parental cancer cells (*$P < 0.05$).

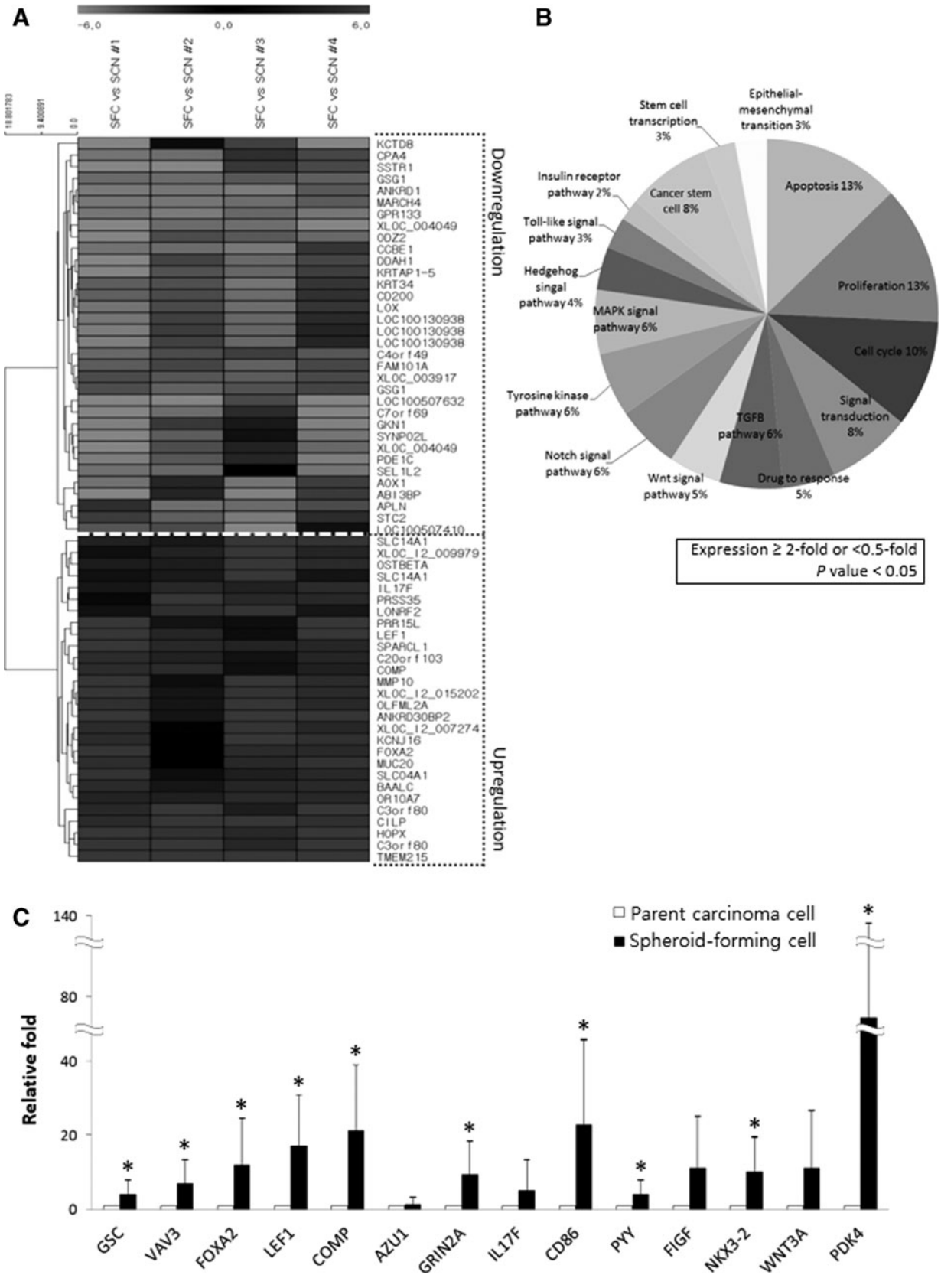
A
-6.0
0.0
6.0
SFC vs SCN #1
SFC vs SCN #2
SFC vs SCN #3
SFC vs SCN #4
KCTD8
CPA4
SSTR1
GSG1
ANKRD1
MARCH4
GPR133
XLOC_004049
ODZ2
CCBE1
DDAH1
KRTAP1-5
KRT34
CD200
LOX
LOC100130938
LOC100130938
LOC100130938
C4orf49
FAM101A
XLOC_003917
GSG1
LOC100507632
C7orf69
GKN1
SYNPO2L
XLOC_004049
PDE1C
SEL1L2
AOX1
ABI3BP
APLN
STC2
LOC100507410
Downregulation
SLC14A1
XLOC_12_009979
OSTBETA
SLC14A1
IL17F
PRSS35
LONRF2
PRR15L
LEF1
SPARCL1
C20orf103
COMP
MMP10
XLOC_12_015202
OLFML2A
ANKRD30BP2
XLOC_12_007274
KCNJ16
FOXA2
MUC20
SLC04A1
BAALC
OR10A7
C3orf80
CILP
HOPX
C3orf80
TMEM215
Upregulation
B
Epithelial-mesenchymal transition 3%
Stem cell transcription 3%
Apoptosis 13%
Insulin receptor pathway 2%
Cancer stem cell 8%
Toll-like signal pathway 3%
Proliferation 13%
Hedgehog singal pathway 4%
MAPK signal pathway 6%
Cell cycle 10%
Tyrosine kinase pathway 6%
Signal transduction 8%
TGFB pathway 6%
Notch signal pathway 6%
Wnt signal pathway 5%
Drug to response 5%
Expression ≥ 2-fold or <0.5-fold
P value < 0.05
C
Parent carcinoma cell
Spheroid-forming cell
Relative fold
140
80
40
20
0
GSC
VAV3
FOXA2
LEF1
COMP
AZU1
GRIN2A
IL17F
CD86
PYY
FIGF
NKX3-2
WNT3A
PDK4

Table 3. Genes Known to be Associated with Oncogenesis and Upregulated More Than 5-Fold in Cancer Stem Cell-Like Cells Compared with Primary Cancer Cells

Genes		*Function*	*Relative fold*	P-*value*
AGT	Angiotensinogen (serpin peptidase inhibitor, clade A, member 8)	SIG	7.13	<0.05
ALDH1A1	Aldehyde dehydrogenase 1 family, member A1	CSC	6.8	<0.05
ANK3	Ankyrin 3, node of Ranvier (ankyrin G)	SIG	8.27	<0.05
AZU1	Azurocidin 1	APO	13.36	<0.05
CD24	CD24 molecule	CSC	13.85	<0.05
CD86	CD86 molecule	PRO	8.67	<0.05
COL15A1	Collagen, type XV, alpha 1	SIG	8.95	<0.05
COMP	Cartilage oligomeric matrix protein	APO	15.34	<0.05
DNAH17	Dynein, axonemal, heavy chain 17	SIG	5.64	<0.05
EGR3	Early growth response 3	SCT	5.36	<0.05
FIGF	c-fos-induced growth factor (vascular endothelial growth factor D)	PRO, SIG, NOT	14.01	<0.05
FOXA2	Forkhead box A2	SIG, SCT	15.11	<0.05
GRIN2A	Glutamate receptor, ionotropic, N-methyl-D-aspartate 2A	SIG, DRU	7.34	<0.05
GSC	Goosecoid homeobox	EMT	8.39	<0.05
HEYL	Hairy/enhancer of split related with YRPW motif-like	EMT, NOT	5.36	<0.05
HGF	Hepatocyte growth factor (hepapoietin A; scatter factor)	EMT, APO, PRO, CYC, SIG	6.66	<0.05
IL17F	Interleukin 17F	SIG	17.36	<0.05
LEF1	Lymphoid enhancer-binding factor 1	EMT, APO, SIG, WNT	28.76	<0.05
MMP10	Matrix metallopeptidase 10 (stromelysin 2)	SIG	25.87	<0.05
NKX3-2	NK3 homeobox 2	APO	9.43	<0.05
NR6A1	Nuclear receptor subfamily 6, group A, member 1	PRO	5.15	<0.05
NTRK2	Neurotrophic tyrosine kinase, receptor, type 2	TYR	5.76	<0.05
NUMB	Numb homolog (*Drosophila*)	NOT	9.13	<0.05
OR10A7	Olfactory receptor, family 10, subfamily A, member 7	SIG	20.94	<0.05
OR1N2	Olfactory receptor, family 1, subfamily N, member 2	SIG	5.15	<0.05
OR2T4	Olfactory receptor, family 2, subfamily T, member 4	SIG	7.02	<0.05
OR9G4	Olfactory receptor, family 9, subfamily G, member 4	SIG	5.37	<0.05
PDGFRB	Platelet-derived growth factor receptor, beta polypeptide	TYR	5.4	<0.05
PDK4	Pyruvate dehydrogenase kinase, isozyme 4	INS, TYR	11.83	<0.05
POU4F1	POU class 4 homeobox 1	SCT	6.84	<0.05
PROC	Protein C (inactivator of coagulation factors, Va and VIIIa)	APO	6.74	<0.05
PYY	Peptide YY	PRO	11.98	<0.05
RASD1	RAS, dexamethasone-induced 1	SIG	5.79	<0.05
SERPINF1	Serpin peptidase inhibitor, clade F, member 1	PRO	6.41	<0.05
SOX2	SRY (sex-determining region Y)-box 2	CSC, SCT	5.36	<0.05
SPEN	Spen homolog, transcriptional regulator (Drosophila)	NOT, TYR, WNT	5.64	<0.05
SYCE1	Synaptonemal complex central element protein 1	CYC	8	<0.05
TNFSF10	Tumor necrosis factor (ligand) superfamily, member 10	SIG, NOT, TGF	6.72	<0.05
TRIL	TLR4 interactor with leucine-rich repeats	TOL	7.19	<0.05
UCN2	Urocortin 2	PRO	6.95	<0.05
VAV3	vav 3 guanine nucleotide exchange factor	SIG	11.75	<0.05
WNT3A	Wingless-type MMTV integration site family, member 3A	PRO, WNT, HED	6.19	<0.05

APO, apoptosis; CSC, cancer stem cell marker; CYC, cell cycle; DRU, drug response; EMT, epithelial–mesenchymal transformation; HED, hedgehog pathway; INS, insulin receptor; NOT, Notch signaling pathway; PRO, proliferation; SCT, stem cell transcription; SIG, signal transduction; TGF, transforming growth factor-β pathway; TOL, Toll-like receptor signaling pathway; TYR, tyrosine kinase signaling; WNT, Wnt pathway.

16% at 24 and 48 h compared with PTX + negative siRNA treatment (Fig. 5C).

Discussion

Ovarian cancer is the most lethal of the gynecological malignancies, and OSC is the predominant and most aggressive subtype of ovarian cancer. Recurrence resulting from chemoresistance occurs in more than 80% of patients with advanced OSC [20], although first-line taxane and platinum-based chemotherapy is initially effective in the majority of patients. Therefore, the mechanisms of recurrence and chemoresistance have been intensively studied, but remain unclear. Ovarian CSCs are believed to be involved in disease relapse [3] as well as in cancer development and chemoresistance; thus, they are considered candidates for biomarkers or novel therapeutic targets [21]. In the present study, to find candidate biomarkers for

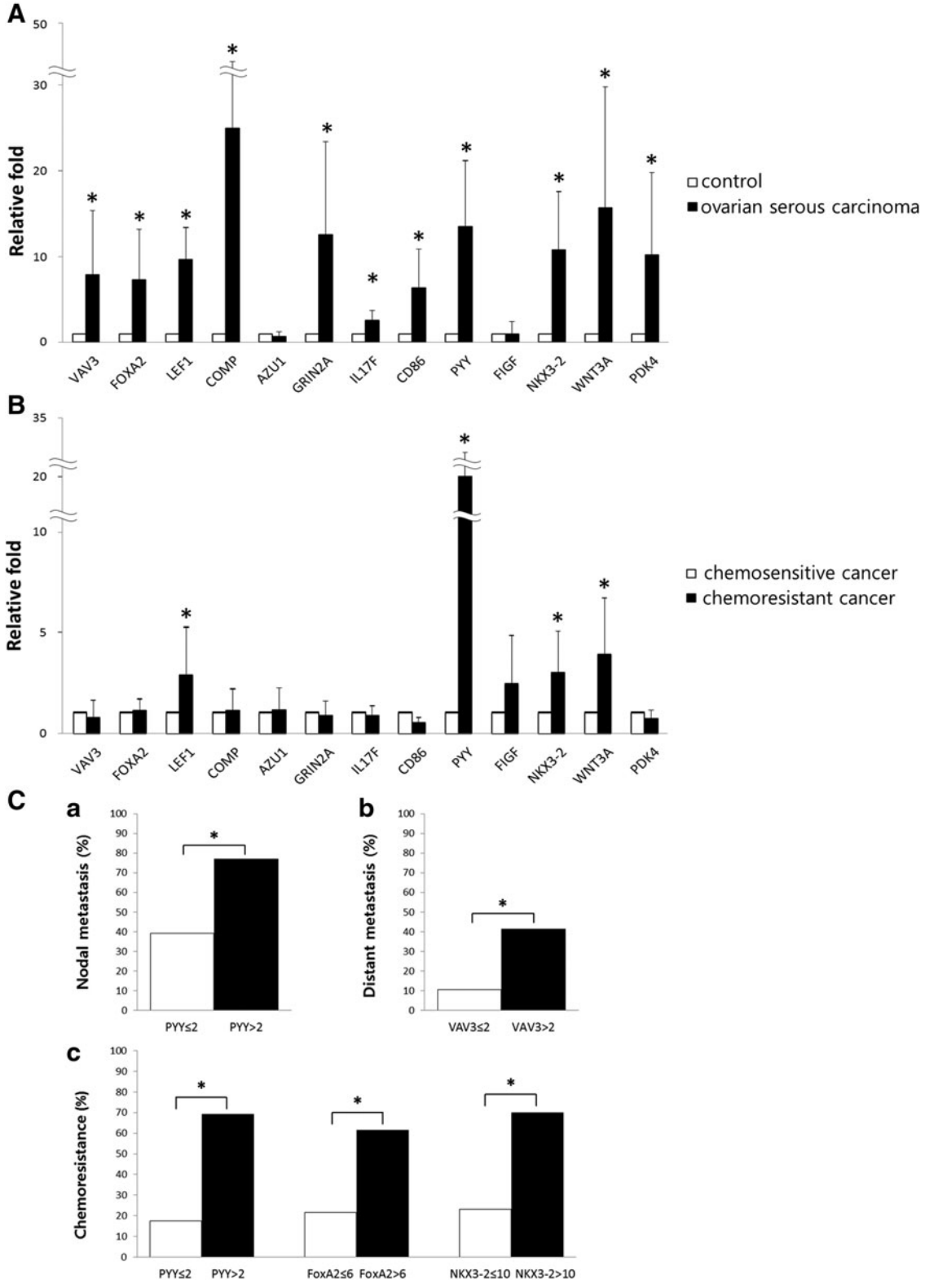

FIG. 3. **(A)** The mRNA expression of selected genes by qRT-PCR. The mRNA levels of 13 genes that were significantly upregulated in SFCs compared with primary cancer cells were evaluated. Eleven genes were significantly overexpressed in OSCs compared with control fallopian tubes (*$P < 0.05$). **(B)** The relative mRNA levels in chemoresistant cancers compared with chemosensitive cancers (*$P < 0.05$). *LEF1*, *PYY*, *NKX3-2*, and *WNT3A* were significantly upregulated in chemoresistant cancers compared with chemosensitive cancers. **(C)** Associations between clinicopathologic parameters and mRNA expression levels by qRT-PCR. **(a)** *PYY* upregulation (>2-fold increase vs. the normal control group) was significantly associated with nodal metastasis (*$P < 0.05$). **(b)** *VAV3* upregulation (>2-fold increase vs. the normal control group) was associated with distant metastasis (*$P < 0.05$). **(c)** The upregulation of *PYY* (>2-fold), *FOXA2* (>6-fold), and *NKX3-2* (>10-fold) each correlated with chemoresistance in OSC (*$P < 0.05$, respectively).

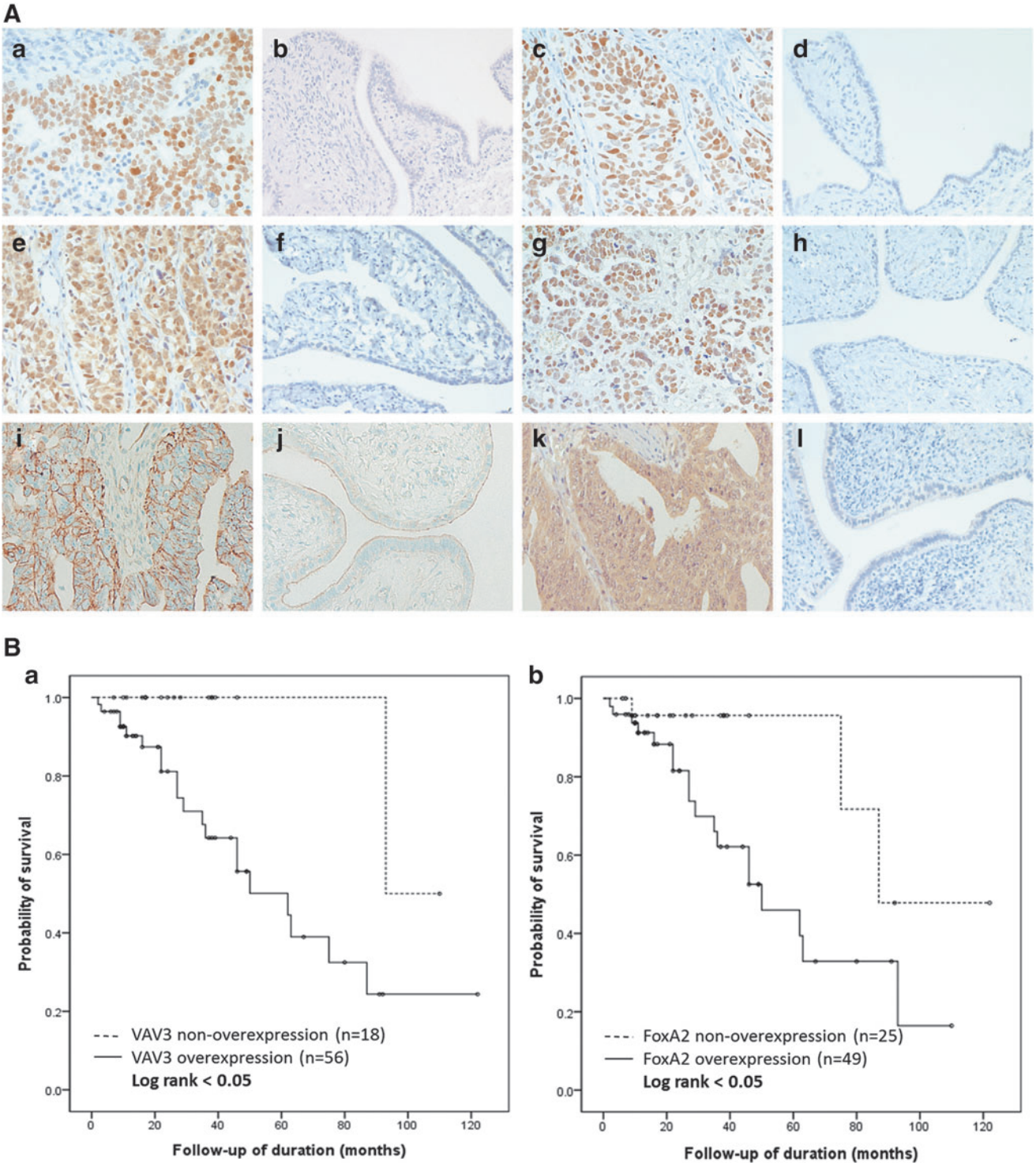

FIG. 4. **(A)** Immunohistochemical staining of OSCs and control tissue. **(a, b)** Positive nuclear staining in OSC, but negative staining in the fallopian tube for FOXA2. **(c, d)** LEF1 showed positive nuclear staining in OSC, but no staining in the fallopian tube. **(e, f)** Positive nuclear and cytoplasmic reactivity for VAV3 in OSC, but not in the fallopian tube. **(g, h)** NKX3-2 staining was observed in the nuclei in OSCs, but not in the fallopian tube. **(i, j)** Membranous staining for Wnt3A was observed in OSC, but only luminal staining was observed in the fallopian tube. **(k, l)** PYY-positive staining in OSC, and negative staining in the fallopian tube. **(B)** Survival curve according to VAV3 and FOXA2 immunohistochemical reactivity. Patients with high levels of VAV3 **(a)** or FOXA2 **(b)** expression showed significantly worse survival than patients with low VAV3 or FOXA2 expression ($P < 0.05$, respectively).

Table 4. Relationships Between Immunohistochemical Expression and Clinicopathologic Parameters in Ovarian Serous Carcinoma ($N=74$)

	FOXA2		*LEF1*		*VAV3*		*PYY*		*NKX3-2*		*Wnt3A*	
	OE	P-*value*	*OE*	P-*value*	*OE*	P-*value*	*OE*	P-*value*	*OE*	P-*value*	*OE*	P-*value*
Age												
<55	24/42	0.059	24/42	0.642	31/42	0.668	25/42	0.777	22/42	0.253	28/42	0.519
≥55	25/32		20/32		25/32		18/32		21/32		19/32	
Clinical stage												
I and II	9/14	0.865	7/14	0.423	9/14	0.270	7/14	0.495	5/14	0.059	10/14	0.494
III and IV	40/60		37/60		47/60		36/60		38/60		37/60	
Nodal metastasis												
Absent	23/35	0.931	19/35	0.390	10/35	0.420	22/35	0.433	19/35	0.528	20/35	0.281
Present	26/39		25/39		31/39		21/39		24/39		27/39	
Distant metastasis												
Absent	24/38	0.568	18/38	**<0.05**[a]	23/38	**<0.05**[a]	24/38	0.366	17/38	**<0.05**[a]	23/38	0.583
Present	25/36		26/36		33/36		19/36		26/36		24/36	
Chemoresistance												
Sensitive	35/55	0.425	31/55	0.356	42/55	0.814	33/55	0.575	28/55	**<0.05**[a]	35/55	0.970
Resistance	14/19		13/19		14/19		10/19		15/19		12/19	

[a], $p<0.05$.

A sample was considered OE when the immunoreactive score was ≥2 for FOXA2; ≥4 for LEF1, PYY, NKX3-2, and Wnt3A; and ≥6 for VAV3.

OE, overexpression.

chemoresistance and poor prognosis and to provide new treatment strategies for life-threatening ovarian cancer, we evaluated the gene expression characteristics of CSCs isolated from human OSC tumors and evaluated their clinical implications using cDNA microarray, qRT-PCR, and IHC staining.

Table 5. Multivariate Cox Regression Analysis for Clinicopathologic Parameters and Immunohistochemical Expression of VAV3 and FOXA2

	No. of cases (n=*74*)	*Death*	*Overall survival*	*Hazard ratio*	P-*value*
Age					
<55	42	9	35.0±29.7	2.38	0.134
≥55	32	12	26.5±23.1		
Clinical stage					
I/II	14	1	38.8±24.2	3.83	0.220
III/IV	60	20	29.6±27.7		
Distant metastasis					
Absent	38	10	38.6±27.1	1.10	0.877
Present	36	11	23.6±25.4		
Chemoresistance					
Sensitive	55	13	37.0±29.1	17.74	**<0.05**[a]
Resistant	19	8	15.0±9.1		
VAV3 expression					
Low	18	1	33.1±27.5	15.27	**<0.05**[a]
High	56	20	30.8±27.3		
FOXA2 expression					
Low	25	3	33.0±30.5	2.51	0.222
High	49	18	30.5±25.6		

[a], $p<0.05$.

The isolation of CSCs was first reported in leukemic cells in 1997 [22], and many other types of CSCs have since been identified. The isolation of CSCs from OSC ascites was first achieved in 2005 [14]; however, high-throughput gene profiling of CSCs isolated from primary tumor tissue has not yet been reported. Numerous methods have been used to isolate putative CSCs, including detection of CSC-specific cell surface markers by flow cytometry, isolation of side population (SP) cells by Hoechst 33342 exclusion, isolation of SFCs in serum-free media, or assessment of aldehyde dehydrogenase activity [3,23–26]. CSCs are usually isolated by flow cytometry using CSC-specific surface markers; however, the subpopulations are difficult to analyze because these surface markers are often nonspecific and because of the low viability of the recovered cells [7]. We therefore isolated putative CSCs using a spheroid formation assay, and spheres were consistently passaged with similar spheroid-forming efficiency in the first and secondary generations. The stemness of these cells was also confirmed by demonstrating overexpression of stem cell markers in second-generation SFCs by qRT-PCR (*ALDH1*, *CD24*, *CD44*, CD133, *NOTCH3*, *SOX2*, and *CD117*), which suggests that CSCs were enriched in isolated SFCs.

There have been many gene expression profiling studies in OSCs [27–29]; however, studies focused on CSCs are very rare and most used cancer cell lines or ascites. Vathipadiekal et al. reported the gene expression profile of SP cells from ascites of patients with advanced-stage OSC [30]. By microarray, 138 genes were upregulated and 302 genes were downregulated in SP cells compared with main population cells. Nineteen genes were randomly selected and validated by qRT-PCR, 7 of which (*ADAM1*, *GEMIN6*, *C6orf153*, *TK2*, *LLGL1*, *FPGT*, and *ST3FAL6*) were overexpressed in recurrent tumors compared with the corresponding primary tumors; however, they did not further

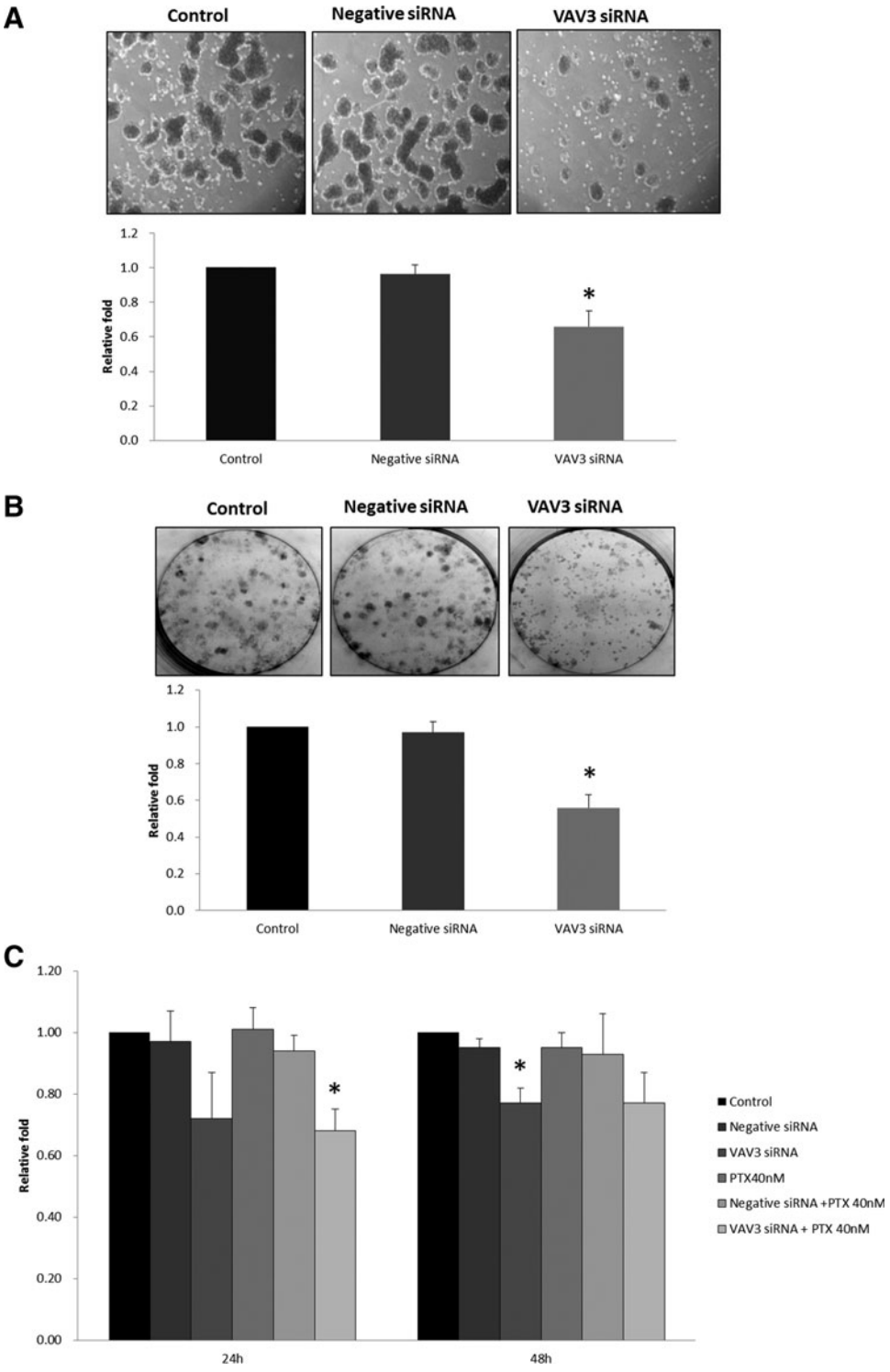

FIG. 5. Effect of *VAV3* knockdown on paclitaxel (PTX)-resistant ovarian cancer cells. **(A)** Spheroid-forming assay. The number of spheroid formations decreased significantly after treatment of *VAV3* siRNA (30% decrease compared with negative siRNA control). The size of the spheroids was also markedly reduced in *VAV3* siRNA-treated SKpac cells compared with that of control and negative siRNA treatment. The graph represents the mean ± standard error of triplicate experiments (*$P <$ 0.001). **(B)** Colony-forming assay. *VAV3* knockdown cells were seeded at 300 cells per well and grown for 14 days. The number of colonies of SKpac cells treated with *VAV3* siRNA decreased by 41% compared with the cells treated with negative siRNA. The graph represents the mean ± standard error of triplicate experiments (*$P <$ 0.001). **(C)** MTT assay. Cell viability was assessed by the MTT assay after inhibition of *VAV3* by siRNA treatment. Cell viability decreased by 25% and 18% (*$P < 0.05$) at 24 and 48 h, respectively, in SKpac cells treated with *VAV3* siRNA compared with the negative siRNA control. With *VAV3* siRNA and 40 nM PTX treatment, the number of SKpac cells decreased by 27% (*$P < 0.05$) and 16% at 24 and 48 h compared with PTX + negative siRNA treatment. The graph represents the mean ± standard error of triplicate experiments.

investigate the clinical implication of these findings with regard to prognosis or patient survival.

In this study, we performed gene expression profiling on CSC-enriched SFCs from OSC primary tumor tissues by cDNA microarray. We then validated the expression of candidate genes by qRT-PCR and IHC using an independent set of OSC samples, and assessed the clinical implications of expression of these genes. To our knowledge, this is the first study to report gene expression profiling of CSCs from the primary tumor bulk of human ovarian carcinomas. Through cDNA microarray and subsequent validation, 14 genes were identified as candidate biomarkers, namely *GSC*, *VAV3*, *FOXA2*, *LEF1*, *COMP*, *AZU1*, *GRIN2A*, *IL17F*, *CD86*, *PYY*, *FIGF*, *NKX3-2*, *WNT3A*, and *PDK4*. Of these genes, GSC was excluded from further validation because we reported it in a previous study [16]. Following qRT-PCR on 36 OSC cases, 11 genes showed significantly higher expression in OSC compared with control tissue (*VAV3*,

FOXA2, *LEF1*, *COMP*, *GRIN2A*, *IL17F*, *CD86*, *PYY*, *NKX3-2*, *WNT3A*, and *PDK4*), and among these genes, *LEF1*, *PYY*, *NKX3-2*, and *WNT3A* were significantly upregulated in chemoresistant cancers compared with chemosensitive cancers. Considering that chemoresistance is related to tumor recurrence, the expression of these genes is expected to be associated with poor prognosis. We therefore studied the protein expression of these genes with an independent validation set of 74 formalin-fixed, paraffin-embedded tumor tissues.

By IHC, overexpression of VAV3, LEF1, and NKX3-2 was significantly associated with distant metastasis, and chemoresistance was significantly related to NKX3-2 overexpression. These results were consistent with the qRT-PCR results showing that *VAV3* upregulation (>2-fold) correlated with distant metastasis and *NKX3-2* upregulation (>10-fold) correlated with chemoresistance. Therefore, we consider VAV3 and NKX3-2 to be candidate markers for the prediction of poor prognosis in OSC patients. In addition, VAV3 overexpression was proved to be an independent poor prognostic factor by multivariate Cox analysis.

VAV3 belongs to the VAV family of proteins [31], which are GDP/GTP guanine nucleotide exchange factors for Rho family GTPases, including RhoA, Racl, and Cdc42. VAV proteins are oncogenes and are involved in numerous cellular signaling pathways [32]. Of the three VAV proteins, VAV3 reportedly plays an important role in tumor development and metastasis [33]. Previous reports demonstrated that VAV3 overexpression was associated with poor prognosis in gastric cancer patients [34], and VAV3 knockdown impaired carcinogenesis in leukemia and gastric cancer [34,35]; however, VAV3 expression in ovarian cancer has not yet been reported. In the present study, we revealed that VAV3 was overexpressed in OSCs, and VAV3 regulated CSC activation and cancer cell proliferation by spheroid-forming and colony-forming assays. We further demonstrated that VAV3 knockdown induced a significant decrease in cell viability of PTX-resistant SKpac cells, representing sensitization of PTX-resistant cancer cells to PTX. To our knowledge, this study is the first to report that VAV3 regulates CSC activation and cell proliferation in ovarian cancer cells and that its overexpression is associated with distant metastasis and worse patient survival.

NKX3-2 is a member of the NK family of proteins and plays a central role in chondrogenic differentiation [36–38]; however, a role for this protein in human cancer has not been reported previously. Our results, which showed that *NKX3-2* was upregulated in OSC and that its overexpression was associated with distant metastasis, imply that NKX3-2 possibly functions as an oncogene in OSC. To confirm this possibility, further functional studies are needed.

LEF1, which showed a significant association with distant metastasis in this study, interacts with β-catenin to form a complex that regulates cell cycle progression and survival [39]. It has been reported to be involved in development and tumorigenesis [40]. Previous studies with ovarian epithelial tumors [41,42] demonstrated a significant change in the expression of some components of the Wnt/Wingless signaling pathway, but the transcriptional activity of Lef-1/β-catenin might play a minor role. FOXA2, another downstream molecule in the Wnt/β-catenin signaling pathway, was associated with poor survival by univariate analysis, although it did not retain its significance on multivariate analysis. FOXA2 is a forkhead transcription factor that is critical during embryogenesis [43,44] and is induced by active Wnt/β-catenin signaling [45]. FOXA2 is associated with an invasive phenotype in primary prostate cancer [46]. Taken together with our findings, Wnt/β-catenin signaling plays a significant role in tumor progression as well as CSC activation in OSCs. Further study is needed to determine the functional implications of LEF1 and FOXA2 in the development and progression of OSC.

In summary, gene expression profiles on CSC-like cells derived from human OSC were generated, and the clinicopathological implications of significantly altered genes were assessed in this study. We found that overexpression of *VAV3* and *NKX3-2* was associated with poor prognosis, including distant metastasis and chemoresistance, and that VAV3 overexpression was an independent poor survival indicator. We further demonstrated that *VAV3* knockdown induced the sensitization of PTX-resistant cancer cells to PTX as well as decrease of CSC activation and cancer cell proliferation. These results suggest that VAV3 is a potential novel biomarker for poor prognosis and a possible therapeutic target in OSC.

Acknowledgment

This research was supported by the Korean government (NRF-2012-R1A1B3004095 and KHIDI-A111804).

Author Disclosure Statement

No competing financial interests exist.

References

1. Lapidot T, C Sirard, J Vormoor, B Murdoch, T Hoang, J Caceres-Cortes, M Minden, B Paterson, MA Caligiuri and JE Dick. (1994). A cell initiating human acute myeloid leukaemia after transplantation into SCID mice. Nature 367:645–648.
2. Kim CF and PB Dirks. (2008). Cancer and stem cell biology: how tightly intertwined? Cell Stem Cell 3:147–150.
3. Ahmed N, K Abubaker, J Findlay and M Quinn. (2013). Cancerous ovarian stem cells: obscure targets for therapy but relevant to chemoresistance. J Cell Biochem 114: 21–34.
4. Conic I, I Dimov, D Tasic-Dimov, B Djordjevic and V Stefanovic. (2011). Ovarian epithelial cancer stem cells. ScientificWorldJournal 11:1243–1269.
5. Dalerba P and MF Clarke. (2007). Cancer stem cells and tumor metastasis: first steps into uncharted territory. Cell Stem Cell 1:241–242.
6. Mor G, G Yin, I Chefetz, Y Yang and A Alvero. (2011). Ovarian cancer stem cells and inflammation. Cancer Biol Ther 11:708–713.
7. Tirino V, V Desiderio, F Paino, A De Rosa, F Papaccio, M La Noce, L Laino, F De Francesco and G Papaccio. (2013). Cancer stem cells in solid tumors: an overview and new approaches for their isolation and characterization. FASEB J 27:13–24.
8. Fong MY and SS Kakar. (2010). The role of cancer stem cells and the side population in epithelial ovarian cancer. Histol Histopathol 25:113–120.

9. Ishii H, M Iwatsuki, K Ieta, D Ohta, N Haraguchi, K Mimori and M Mori. (2008). Cancer stem cells and chemoradiation resistance. Cancer Sci 99:1871–1877.
10. Valent P, D Bonnet, R De Maria, T Lapidot, M Copland, JV Melo, C Chomienne, F Ishikawa, JJ Schuringa, et al. (2012). Cancer stem cell definitions and terminology: the devil is in the details. Nat Rev Cancer 12:767–775.
11. Vang R, M Shih Ie and RJ Kurman. (2009). Ovarian low-grade and high-grade serous carcinoma: pathogenesis, clinicopathologic and molecular biologic features, and diagnostic problems. Adv Anat Pathol 16:267–282.
12. Lee DH, K Chung, JA Song, TH Kim, H Kang, JH Huh, SG Jung, JJ Ko and HJ An. (2010). Proteomic identification of paclitaxel-resistance associated hnRNP A2 and GDI 2 proteins in human ovarian cancer cells. J Proteome Res 9:5668–5676.
13. He QZ, XZ Luo, K Wang, Q Zhou, H Ao, Y Yang, SX Li, Y Li, HT Zhu and T Duan. (2014). Isolation and characterization of cancer stem cells from high-grade serous ovarian carcinomas. Cell Physiol Biochem 33: 173–184.
14. Bapat SA, AM Mali, CB Koppikar and NK Kurrey. (2005). Stem and progenitor-like cells contribute to the aggressive behavior of human epithelial ovarian cancer. Cancer Res 65:3025–3029.
15. Baba T, PA Convery, N Matsumura, RS Whitaker, E Kondoh, T Perry, Z Huang, RC Bentley, S Mori, et al. (2009). Epigenetic regulation of CD133 and tumorigenicity of CD133+ ovarian cancer cells. Oncogene 28:209–218.
16. Kang KW, MJ Lee, JA Song, JY Jeong, YK Kim, C Lee, TH Kim, KB Kwak, OJ Kim and HJ An. (2014). Overexpression of goosecoid homeobox is associated with chemoresistance and poor prognosis in ovarian carcinoma. Oncol Rep 32:189–198.
17. Karst AM and R Drapkin. (2010). Ovarian cancer pathogenesis: a model in evolution. J Oncol 2010:932371.
18. Leeper K, R Garcia, E Swisher, B Goff, B Greer and P Paley. (2002). Pathologic findings in prophylactic oophorectomy specimens in high-risk women. Gynecol Oncol 87:52–56.
19. Medeiros F, MG Muto, Y Lee, JA Elvin, MJ Callahan, C Feltmate, JE Garber, DW Cramer and CP Crum. (2006). The tubal fimbria is a preferred site for early adenocarcinoma in women with familial ovarian cancer syndrome. Am J Surg Pathol 30:230–236.
20. Armstrong A, B Otvos, S Singh and R Debernardo. (2013). Evaluation of the cost of CA-125 measurement, physical exam, and imaging in the diagnosis of recurrent ovarian cancer. Gynecol Oncol 131:503–507.
21. Clarke MF and M Fuller. (2006). Stem cells and cancer: two faces of eve. Cell 124:1111–1115.
22. Bonnet D and JE Dick. (1997). Human acute myeloid leukemia is organized as a hierarchy that originates from a primitive hematopoietic cell. Nat Med 3:730–737.
23. Avital I, A Stojadinovic, H Wang, C Mannion, WC Cho, J Wang and YG Man. (2014). Isolation of stem cells using spheroids from fresh surgical specimen: an analytic minireview. Cancer Genomics Proteomics 11:57–65.
24. Bapat SA. (2010). Human ovarian cancer stem cells. Reproduction 140:33–41.
25. Shi MF, J Jiao, WG Lu, F Ye, D Ma, QG Dong and X Xie. (2010). Identification of cancer stem cell-like cells from human epithelial ovarian carcinoma cell line. Cell Mol Life Sci 67:3915–3925.
26. Szotek PP, R Pieretti-Vanmarcke, PT Masiakos, DM Dinulescu, D Connolly, R Foster, D Dombkowski, F Preffer, DT Maclaughlin and PK Donahoe. (2006). Ovarian cancer side population defines cells with stem cell-like characteristics and Mullerian Inhibiting Substance responsiveness. Proc Natl Acad Sci U S A 103:11154–11159.
27. Donninger H, T Bonome, M Radonovich, CA Pise-Masison, J Brady, JH Shih, JC Barrett and MJ Birrer. (2004). Whole genome expression profiling of advance stage papillary serous ovarian cancer reveals activated pathways. Oncogene 23:8065–8077.
28. Fehrmann RS, XY Li, AG van der Zee, S de Jong, GJ Te Meerman, EG de Vries and AP Crijns. (2007). Profiling studies in ovarian cancer: a review. Oncologist 12:960–966.
29. Gomez-Raposo C, M Mendiola, J Barriuso, D Hardisson and A Redondo. (2010). Molecular characterization of ovarian cancer by gene-expression profiling. Gynecol Oncol 118:88–92.
30. Vathipadiekal V, D Saxena, SC Mok, PV Hauschka, L Ozbun and MJ Birrer. (2012). Identification of a potential ovarian cancer stem cell gene expression profile from advanced stage papillary serous ovarian cancer. PLoS One 7:e29079.
31. Lee K, Y Liu, JQ Mo, J Zhang, Z Dong and S Lu. (2008). Vav3 oncogene activates estrogen receptor and its overexpression may be involved in human breast cancer. BMC Cancer 8:158.
32. Katzav S, D Martin-Zanca and M Barbacid. (1989). vav, a novel human oncogene derived from a locus ubiquitously expressed in hematopoietic cells. EMBO J 8:2283–2290.
33. Fernandez-Salguero PM. (2010). A remarkable new target gene for the dioxin receptor: the Vav3 proto-oncogene links AhR to adhesion and migration. Cell Adh Migr 4:172–175.
34. Lin KY, LH Wang, YC Hseu, CL Fang, HL Yang, KJ Kumar, C Tai and YH Uen. (2012). Clinical significance of increased guanine nucleotide exchange factor Vav3 expression in human gastric cancer. Mol Cancer Res 10:750–759.
35. Chang KH, A Sanchez-Aguilera, S Shen, A Sengupta, MN Madhu, AM Ficker, SK Dunn, AM Kuenzi, JL Arnett, et al. (2012). Vav3 collaborates with p190-BCR-ABL in lymphoid progenitor leukemogenesis, proliferation, and survival. Blood 120:800–811.
36. Cairns DM, R Liu, M Sen, JP Canner, A Schindeler, DG Little and L Zeng. (2012). Interplay of Nkx3.2, Sox9 and Pax3 regulates chondrogenic differentiation of muscle progenitor cells. PLoS One 7:e39642.
37. Herbrand H, O Pabst, R Hill and HH Arnold. (2002). Transcription factors Nkx3.1 and Nkx3.2 (Bapx1) play an overlapping role in sclerotomal development of the mouse. Mech Dev 117:217–224.
38. Lettice L, J Hecksher-Sorensen and R Hill. (2001). The role of Bapx1 (Nkx3.2) in the development and evolution of the axial skeleton. J Anat 199:181–187.
39. Behrens J, JP von Kries, M Kuhl, L Bruhn, D Wedlich, R Grosschedl and W Birchmeier. (1996). Functional interaction of beta-catenin with the transcription factor LEF-1. Nature 382:638–642.
40. Novak A and S Dedhar. (1999). Signaling through beta-catenin and Lef/Tcf. Cell Mol Life Sci 56:523–537.
41. Lee CM, H Shvartsman, MT Deavers, SC Wang, W Xia, R Schmandt, DC Bodurka, EN Atkinson, A Malpica, et al. (2003). beta-catenin nuclear localization is associated with grade in ovarian serous carcinoma. Gynecol Oncol 88:363–368.

42. Rask K, A Nilsson, M Brannstrom, P Carlsson, P Hellberg, PO Janson, L Hedin and K Sundfeldt. (2003). Wnt-signalling pathway in ovarian epithelial tumours: increased expression of beta-catenin and GSK3beta. Br J Cancer 89:1298–1304.
43. Friedman JR and KH Kaestner. (2006). The Foxa family of transcription factors in development and metabolism. Cell Mol Life Sci 63:2317–2328.
44. Kaestner KH. (2010). The FoxA factors in organogenesis and differentiation. Curr Opin Genet Dev 20:527–532.
45. Yu X, Y Wang, DJ DeGraff, ML Wills and RJ Matusik. (2011). Wnt/beta-catenin activation promotes prostate tumor progression in a mouse model. Oncogene 30:1868–1879.
46. Mirosevich J, N Gao, A Gupta, SB Shappell, R Jove and RJ Matusik. (2006). Expression and role of Foxa proteins in prostate cancer. Prostate 66:1013–1028.

Address correspondence to:
Dr. Hee Jung An
Department of Pathology
College of Medicine
CHA University
351 Yatap-Dong
Bundang-Gu
Sungnam
Gyeonggi-Do 463-712
Republic of Korea

E-mail: hjahn@cha.ac.kr

Received for publication December 23, 2014
Accepted after revision February 10, 2015
Prepublished on Liebert Instant Online February 25, 2015